Phosphatidylinositol-4,5-Biphosphate-Dependent Rearrangement of TRPV4 Cytosolic Tails Enables Channel Activation by Physiological Stimuli

PIP_2-DEPENDENT REARRANGEMENT OF TRPV4 CYTOSOLIC TAILS ENABLES CHANNEL ACTIVATION BY PHYSIOLOGICAL STIMULI

Anna Garcia-Elias[a,1], Sanela Mrkonjić[a,1], Carlos Pardo-Pastor[a], Hitoshi Inada[b], Ute A. Hellmich[b], Fanny Rubio-Moscardó[a], Cristina Plata[a], Rachelle Gaudet[b], Rubén Vicente[a] and Miguel A. Valverde[a,2]

[a]Laboratory of Molecular Physiology and Channelopathies,Dept. of Experimental and Health Sciences, Universitat Pompeu Fabra, Barcelona, Spain; [b]Dept. of Molecular and Cellular Biology, Harvard University, Cambridge, USA.

Submitted to Proceedings of the National Academy of Sciences of the United States of America

Most TRP channels are regulated by phosphatidylinositol-4,5-biphosphate (PIP_2), although the structural rearrangements occurring upon PIP_2 binding are currently far from being understood. Here we report that TRPV4 activation by hypotonic and heat stimuli requires PIP_2 binding to and rearranging of the cytosolic tails. Neutralization of the positive charges within the sequence ^{121}KRWRK^{125}, which resembles a phosphoinositide binding site, rendered the channel unresponsive to hypotonicity and heat but responsive to 4α-phorbol 12,13-didecanoate, an agonist that binds directly to transmembrane domains. Similar channel response was obtained by depleting PIP_2 from the plasma membrane with translocatable phosphatases in heterologous expression systems or by activation of phospholipase C in native ciliated epithelial cells. PIP_2 facilitated TRPV4 activation by the osmotransducing cytosolic messenger 5'-6'-epoxyeicosatrienoic acid and allowed channel activation by heat in inside-out patches. Protease protection assays demonstrated a PIP_2 binding site within the N-tail. The proximity of TRPV4 tails, analysed by fluorescence resonance energy transfer, increased by depleting PIP_2, mutations in the PI-site or by co-expression with PACSIN3, a regulatory molecule that binds TRPV4 N-tails and abrogates activation by cell swelling and heat. PACSIN3 lacking the F-BAR domain interacted with TRPV4 without affecting channel activation or tail rearrangement. Therefore, mutations weakening the TRPV4-PIP_2 interacting site and conditions that deplete PIP_2 or restrict TRPV4 access to PIP_2 –in the case of PACSIN3- change tail conformation and negatively affect channel activation by hypotonicity and heat.

TRP | conformational change | heat | osmotic

INTRODUCTION

TRPV4 is a non-selective cation channel that responds to osmotic (1-4), mechanical (5-7) and temperature stimulation (8), thereby contributing to many different physiological functions: cellular (4, 9) and systemic volume homeostasis (10), vasodilation (11, 12), nociception (13), epithelial hydroelectrolyte transport (14), bladder voiding (15), ciliary beat frequency regulation (7, 16, 17), chondroprotection (18) and skeletal regulation (19). Osmotic (20) and mechanical (7, 16) sensitivity of TRPV4 depends on phospholipase A_2 activation and the subsequent production of the arachidonic acid metabolites, epoxyeicosatrienoic acids (EET), while the mechanism leading to temperature-mediated activation (only observed in intact cells) it is not known at present (21). Reports also exists claiming EET-independent TRPV4 activation by membrane stretch in excised-patches from oocytes (22), in apparent contradiction with early reports claiming lack of activation by membrane stretch (1). Several studies have characterized TRPV4 domains implicated in channel regulation by calmodulin (23, 24), PACSIN3 (25), intracellular ATP (24) and inositol-trisphosphate receptor (16, 26). However, little is known about the domains relevant for TRPV4 activation by different stimuli, apart from the interaction between the TRPV4 activator 4α-phorbol 12,13-didecanoate (4α−PDD) and transmembrane domains 3 and 4 (27). Analysis of disease-causing mutations modifying channel activity that lay in regions close to the channel pore or within the ankyrin repeats (28) has also contributed to our understanding of relevant protein domains.

Most TRP channels are regulated by phosphatidylinositol phosphates, particularly by phosphatidylinositol-4,5-biphosphate (PIP_2), which is the most abundant phosphoinositide in the inner leaflet of the plasma membrane (29, 30). In general terms, it is proposed that PIP_2 modulates TRP channel gating and/or the sensitivity to activating stimuli (29, 30). The interaction of PIP_2 with TRPs involves protein regions characterised by the presence of several positively charged residues. Mutations of these positive residues (31-33) and manipulation of the PIP_2 levels in intact cells (34) or in excised patches (33) have been the main tools to evaluate PIP_2-mediated channel regulation.

The recent report of the crystal structure of K^+ channels with bound PIP_2 provides the first atomistic description of a molecular mechanism by which PIP_2 regulates channel activity (35, 36). PIP_2 binding induces a large conformation change in the protein, expanding and bringing the cytosolic domains closer to the transmembrane domains (35). Whether PIP_2 modulation of TRP channels involves similar conformational changes is still an open question.

We now show that TRPV4 requires the interaction of PIP_2 with a stretch of positive charges at the N-tail, prior to the proline-rich domain (PRD, residues 132-144), in order to be activated by hypotonicity and heat. Moreover, we have also demonstrated that the reported lack of channel response to heat in excised patches is fully recovered in the presence of PIP_2, thereby suggesting that TRPV4 is *bona fide* thermosensitive channel. Finally, reduction of PIP_2 levels or disruption of the PIP_2 interaction with the channel increased FRET signal between fluorescent probes on the TRPV4 cytosolic tails, consistent with a more compact cytosolic region. This is the first piece of evidence suggesting that, similar to PIP_2-regulated K^+ channels, PIP_2 interaction with the TRPV4 channel rearranges cytosolic domains.

RESULTS AND DISCUSSION

A possible phosphoinositide interacting site in the TRPV4 N-tail is required for channel activation by hypotonicity and heat. We

Reserved for Publication Footnotes

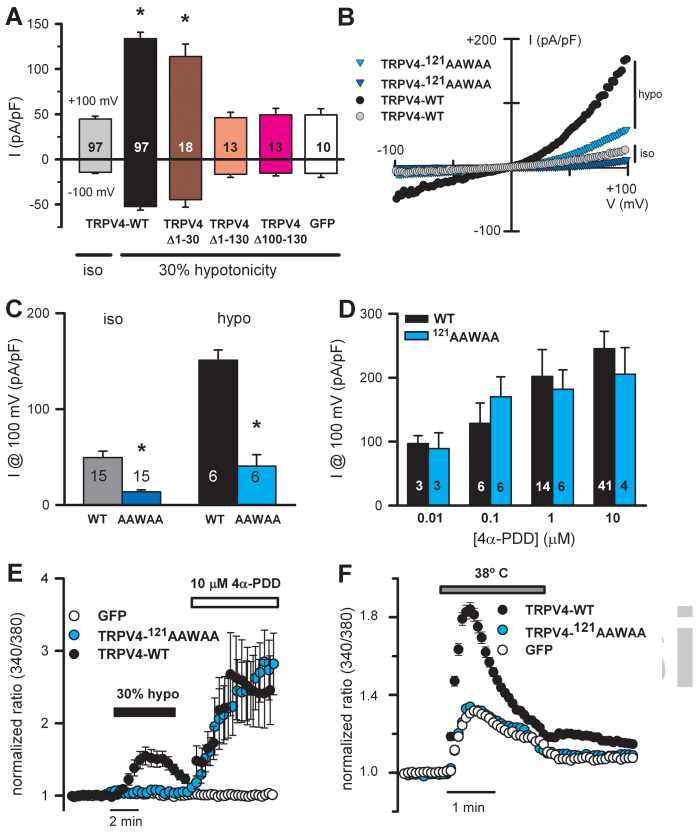

Fig. 1. Functional analysis of N-terminal truncations and mutations of TRPV4. (A)Mean current density measured at +100 and -100 mV in response to a 30% hypotonic shock in HEK-293 cells overexpressing TRPV4-WT, TRPV4-Δ1-30, TRPV4-Δ1-130, TRPV4-Δ100-130 and GFP.Number of cells recorded is shown for each condition.(B)Ramp current-voltage relations of cationic currents recorded from HEK-293 cells transfected with TRPV4-WT or TRPV4-^{121}AAWAA and exposed to 30% hypotonic shocks. (C) Mean current responses to isotonic and hypotonic stimuli in cells transfected with TRPV4-WT or TRPV4-^{121}AAWAA. (D) Mean current responses to 4α-PDD stimulation in TRPV4-WT or TRPV4-^{121}AAWAA expressing cells. (E) Calcium signals (Fura-2 ratio) obtained in HeLa cells transfected with GFP (n=47), TRPV4-WT (n=25) or TRPV4-^{121}AAWAA (n=59) and sequentially stimulated with 30% hypotonic solutions and 10 μM 4αPDD. (F) Calcium signals obtained in HeLa cells transfected with TRPV4-WT (n=335), TRPV4-^{121}AAWAA (n=318) or GFP (n=254) and stimulated with warm solutions (38ºC). * P<0.05.

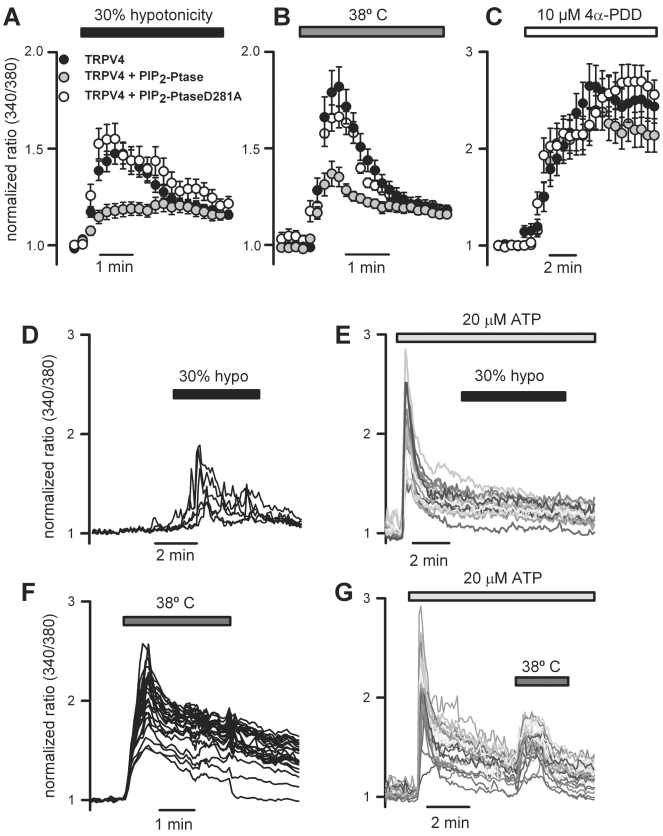

Fig. 2. . Effect of PIP_2 depletion on TRPV4-mediated Ca^{2+} signals. HeLa cells were transfected with TRPV4-WT, TRPV4-WT plus FRB and FKBP-5-phosphatase (PIP_2-ptase) or the inactive phosphatase (D281A). (A-C) Average calcium signals (fura-2 ratio) measured in the presence of the phosphatase translocation inducing agent rapamycin (1 μM) for cells exposed to (A) 30% hypotonicity (TRPV4, n=302; V4+PIP_2-Ptase, n=229; V4+PIP_2-PtaseD281A, n=192), (B) heat (TRPV4, n=150; V4+PIP_2-Ptase, n=146; V4+PIP_2-PtaseD281A, n=89) and (C) 4α-PDD (TRPV4, n=278; V4+PIP_2-Ptase, n=233; V4+PIP_2-PtaseD281A, n=89). (D-G) Representative intracellular Ca^{2+} signals obtained from mouse tracheal ciliated cells exposed to a hypotonic solution in the absence (D) or the presence (E) of 20 μM ATP, or exposed to heat (38ºC) in the absence (F) or the presence (G) of 20 μM ATP. Percentage of ciliated cells responding to hypotonicity and heat was >90%. In the presence of ATP the percentages were <5% (hypotonicity) and >90% (heat).

screened TRPV4 for domains that may participate in the channel response to hypotonicity-induced cell swelling. A schematic view of the channel molecule and all deletions/mutations generated is shown in Supporting Information Fig. S1. We focused on the N-terminus tail because a TRPV4 SNP associated with hyponatremia, P19S, generates a channel with reduced response to hypotonic cell swelling (37). We generated three deletions of different length: TRPV4-Δ1-30, TRPV4-Δ1-130 and TRPV4-Δ100-130.

TRPV4 sensitivity to hypotonic conditions was assayed using whole-cell patch clamp recordings and intracellular calcium imaging with fura-2. Addition of a 30% hypotonic solution yielded large currents in cells transiently transfected with TRPV4-WT but not in GFP-transfected cells (Fig. S2A). TRPV4-Δ1-130 and TRPV4-Δ100-130 responses to 30% hypotonicity were reduced to the levels recorded in GFP-transfected cells while TRPV4-Δ1-30 displayed a normal response (Fig. 1A and Fig. S2B). Deletion of the first 30 residues did greatly reduce currents generated by 15% hypotonic solutions (Fig. S2D), mimicking the changes induced by the P19S polymorphism (37). Consistent with the electrophysiological experiments, expression of TRPV4-WT increased intracellular [Ca^{2+}] in response to 30% hypotonicity while the response of TRPV4-Δ100-130 was indistinguishable from that obtained in GFP-transfected cells (Fig. S2C). To evaluate if differences in plasma membrane expression between WT and mutant TRPV4 proteins could explain the reduced responses of truncated TRPV4 proteins we determined surface labeling of HEK-293 cells expressing TRPV4-WT and TRPV4-Δ1-130 proteins tagged with a V5 epitope in the first extracellular loop. Confocal microscopy images and quantification by ELISA revealed no apparent differences in membrane expression between TRPV4-WT and the protein presenting the longest truncation, TRPV4-Δ1-130 (Fig. S3).

To pin down the region within residues 100-130 required for the channel response to hypotonic cell swelling we neutralized four positive charges within a sequence (^{121}KRWRK^{125}) that has been proposed to be a possible phosphoinositide binding site (PI-site) (29). Cells transfected with TRPV4-^{121}AAWAA displayed greatly reduced swelling-induced whole-cell cationic currents (Fig. 1B-C). TRPV4-^{121}AAWAA generated currents in response to the synthetic agonist 4α−PDD (0.01-10 μM) were undistinguishable from TRPV4-WT currents (Fig. 1D). Sequential addition of a hypotonic solution and 10 μM 4α−PDD generated

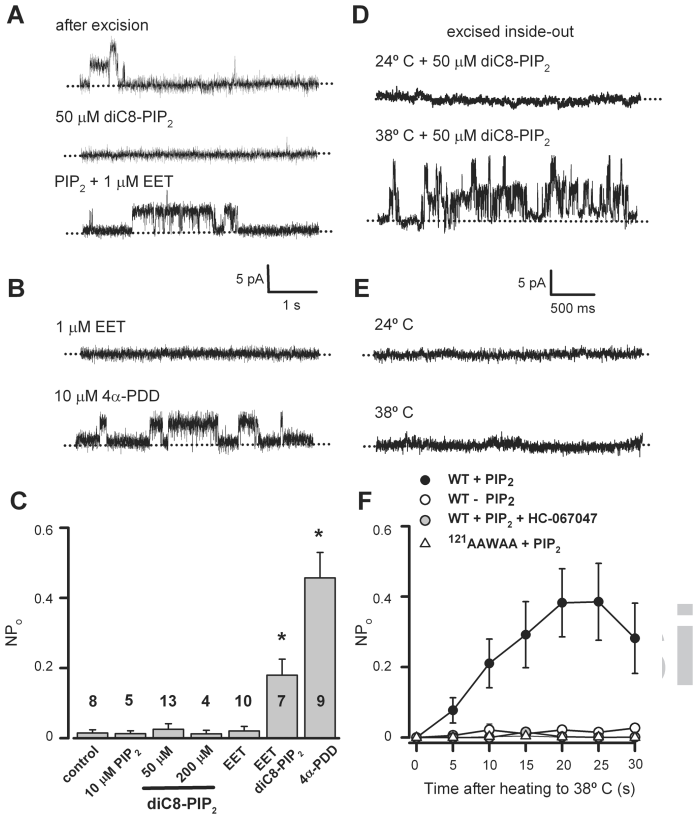

Fig. 3. Effect of PIP_2 on TRPV4 channel activity in inside-out patches. (A) Two TRPV4 single-channel openings, which disappeared within seconds, were observed at +80 mV immediately after excision of a HeLa cell membrane patch (top). Addition of diC8-PIP_2 (50 μM) after complete channel rundown did not reactivate TRPV4 (middle) while addition of 5,6-EET (1 μM) in the presence of PIP_2 activated TRPV4 (bottom). (B) Recordings obtained at +80 mV in a patch sequentially exposed to EET (1 μM) and 4α-PDD (10 μM). (C), Mean open probability (NP_o) calculated from control patches (2 min after excision) and in response to PIP_2, EET, EET+PIP_2 and 4α-PDD (number of patches given in the figure). Percentages patches presenting TRPV4 activity: PIP_2 20%, EET 20%, EET+PIP_2 71% and 4α-PDD 88%. (D-E) Single channel recordings obtained from the same excised patch in response to 24ºC and warm solutions (38ºC) in the presence (D) or in the absence (E) of 50 μM diC8-PIP_2. (F), NP_o calculated from consecutive 5 sec recordings following exposure to warm solutions and plotted versus time (+PIP_2, n=11; -PIP_2, n=7; +PIP_2 +1 μM HC-067047 (in pipette solution), n=4; TRPV4-^{121}AAWAA + PIP_2, n=5). * P<0.05.

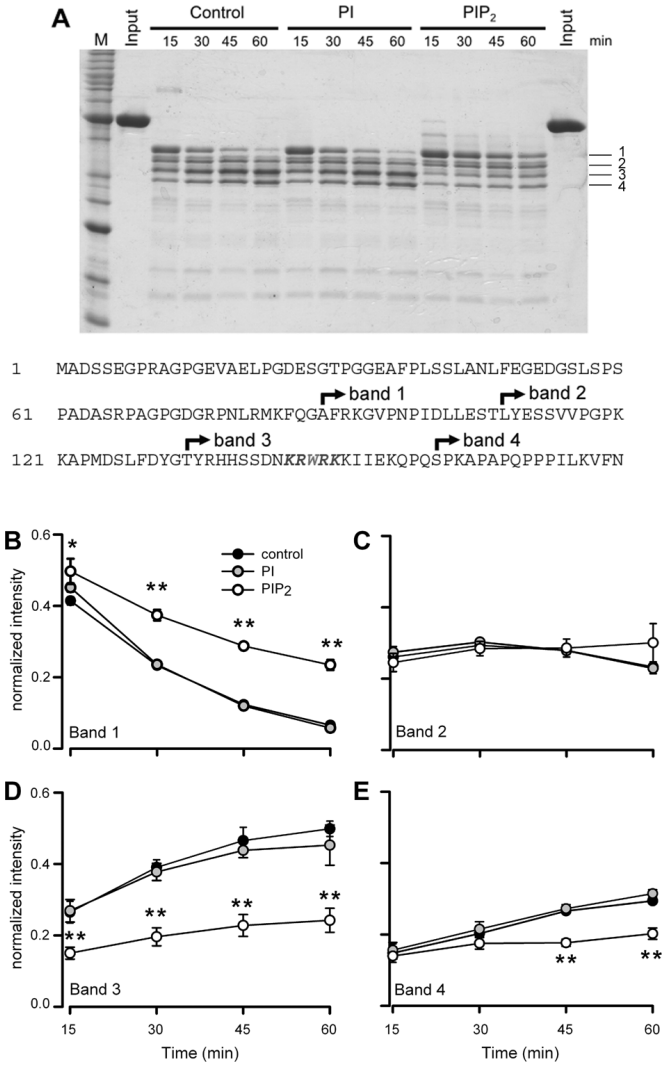

Fig. 4. PIP_2 binding to the TRPV4 N-tail. (A), Coomassie-stained SDS-PAGE showing protection from limited papain digestion by PIP_2 but not PI. Purified protein corresponding to residues 1-397 of human TRPV4 (150 μM) was digested with papain (38 nM) in the absence or presence of lipid (PI and PIP_2 at 10 μM). The cleavage positions corresponding to each isolated band, determined by N-terminal sequencing, are indicated. (B-E) The four indicated bands were scanned, quantified and plotted *versus* digestion time. Significant changes were observed in the presence of PIP_2 for bands 1 and 3 at all times while band 4 showed significant differences at time 45 and 60 min. Mean±S.D. (n=3). * P<0.05 control *vs* PIP_2 ; ** P<0.01 control and PI *vs* PIP_2.

significant increases in intracellular Ca^{2+} levels in cells expressing TRPV4-WT while cells expressing TRPV4-^{121}AAWAA only responded to 4α−PDD (Fig. 1E).

TRPV4 is also activated by moderate heat (above 25ºC) (8, 21), although the mechanism of its temperature sensitivity is not fully understood (8). Ca^{2+} imaging on cells exposed to warm temperatures (38ºC) revealed a typical transient response in cells transfected with TRPV4-WT channels. Neutralization of the positive charges in the TRPV4-^{121}AAWAA decreased the Ca^{2+} response to the levels obtained in GFP-transfected cells (Fig. 1F).

We hypothesized that the sequence ^{121}KRWRK^{125} may form a PI-site required for phosphatidylinositol-4,5-biphosphate (PIP_2) interaction with TRPV4 to respond to hypotonic and heat stimulation. Different TRP protein sequences containing several positively charged amino acids have been proposed to interact with phosphoinositides, particularly PIP_2 (29, 38). To examine how specific was the neutralization of the ^{121}KRWRK^{125} positive charges, we neutralized three positive charges of a nearby region (^{114}RHH^{116}). Expression of TRPV4-^{114}AAA produced hypotonicity and heat-induced Ca^{2+} increases similar to those obtained with TRPV4-WT (Fig S4A). Together, these experiments suggested that residues ^{121}KRWRK^{125} are critical for TRPV4 activation by hypotonicity and heat, but not necessary for channel activation by 4α−PDD.

Depletion of PIP_2 levels prevents channel activation by physiological stimuli. We assessed whether deletion or mutation of residues ^{121}KRWRK^{125} may be related to a PIP_2-dependent mode of TRPV4 gating. For that purpose, we evaluated the impact of reducing PIP_2 levels on channel activation. We used a rapamycin-induced translocatable 5-phosphatase to deplete PIP_2 (39). The membrane-localized rapamycin-binding protein FRB and the cytoplasmic enzyme construct FKBP-5-phosphatase were co-transfected with TRPV4-WT in HeLa cells. Addition of

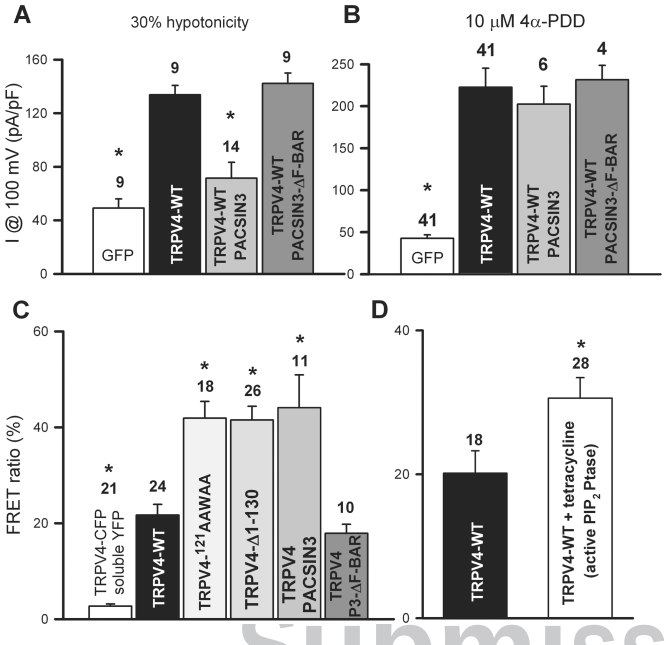

Fig. 5. PIP_2-dependent rearrangment of TRPV4 cytosolic tails. (A-B), Mean current density of hypotonicity-activated (A) or 4α-PDD-activated (B) currents recorded from HEK-293 cells transfected with GFP, TRPV4, TRPV4+PACSIN3 or TRPV4+PACSIN3-ΔF-BAR. (C) FRET efficiency was determined at the plasma membrane of HEK-293 coexpressing soluble YFP and CFP-fused TRPV4, CFP- and YFP-fused TRPV4-WT, CFP- and YFP-fused TRPV4-^{121}AAWAA, CFP- and YFP-fused TRPV4-Δ1-130, or CFP- and YFP-fused TRPV4-WT coexpressed with either PACSIN3 or PACSIN3-ΔF-BAR. (D) FRET efficiencies between CFP- and YFP-fused TRPV4-WT determined at the plasma membrane in the absence or presence of tetracyclin. TRPV4 constructs were transiently cotransfected in HEK-293 cells expressing a tetracyclin-inducible 5-phosphatase. Number of cells recorded is shown for each condition. Mean±S.E.M. * $P<0.05$ *versus* TRPV4-WT, one way ANOVA and Bonferroni *post hoc* (A-C) or Student's t test (D).

rapamycin to translocate the phosphatase to the plasma membrane, locally depleted membrane PIP_2 (Fig. S5A-C) and prevented the increase of the Ca^{2+} signal following hypotonic cell swelling (Fig. 2A) and heat stimulation (Fig. 2B) without affecting the response to 0.1-10 μM 4α-PDD (Fig. 2C; and Fig. S4B). Application of rapamycin to cells cotransfected with TRPV4 and a phosphatase-dead mutant (D281A) (39) did not affect the Ca^{2+} response to any of the stimuli tested (Fig. 2A-C).

We also analyzed whether phospholipase C (PLC)-induced depletion of PIP_2 decreased TRPV4 channel activity in native cells. For that purpose we used primary cultures of ciliated epithelial cells obtained from trachea and oviduct, which express functional TRPV4 channels (7, 16, 17). Figure 2D shows typical oscillatory Ca^{2+} signals generated by hypotonic solutions in tracheal ciliated epithelial cells. However, Ca^{2+} response to hypotonicity was abrogated following the activation of PLC with ATP, which leads to the hydrolysis of PIP_2 and the generation of an IP_3-mediated Ca^{2+} signal (Fig. 2E). The heat response of epithelial cells was also reduced following the addition of ATP (Fig. 2F-G). The reduction in hypotonicity- and heat-induced Ca^{2+} signal were not due to Ca^{2+}-dependent inhibition of TRPV4 as two consecutive stimuli elicited similar responses (Fig. S6A-B). Similarly, mouse ciliated oviductal cells responses to hypotonicity were reduced following addition of ATP (Fig. S6C-D). Although we could not asses directly whether PIP_2 remained depleted at the time cells were challenged with TRPV4 activating stimuli, the fact that there was no Ca^{2+} response to a second ATP stimulation within minutes of the first ATP application (Fig. S6E) may reflect a condition of PIP_2 depletion.

Activity of PIP_2-regulated channels typically decreases in excised inside-out patches and recovers upon addition of exogenous PIP_2 (40). In those excised patches in which TRPV4 channel activity was present immediately after excision, channel activity decreased with time and addition of the water soluble diC8-PIP_2 (50-200 μM) or long acyl chain PIP_2 (10 μM) did not recover initial channel activity (Fig. 3A and C). The fact that PIP_2 was not able to activate TRPV4 in excised patches may indicate that following patch excision another, yet unidentified, modulator required for channel activity is lost. Hypotonicity-mediated activation of TRPV4 in excised patches can not be directly evaluated. Instead, the osmotransducing cytosolic messenger 5'-6'-epoxyeicosatrienoic acid (EET) has been used (20, 41). Addition of EET (1 μM) in the presence of PIP_2 activated TRPV4 in 71% of patches (Fig. 3A and C). However, addition of EET in the absence of PIP_2 only activated 20 % of patches (Fig. 3B and C), even though TRPV4 channel activity in the same patches was demonstrated using 4α−PDD (Fig. 3B).

Next, we tested channel activation by heat in excised inside-out patches obtained from HeLa cells overexpressing TRPV4. In the presence of PIP_2 TRPV4-WT channel activity was detected within seconds after application of warm solutions (Fig. 3D) while in the presence of PIP_2 and the TRPV4 blocker HC-067047 (42) or with the TRPV4-^{121}AAWAA no channel activity was elicited by heat (Fig. 3F). We discarded a shear-stress dependent component under our experimental conditions for heat activation of TRPV4 (Fig. S7A). In the absence of PIP_2, and consistent with previous reports (8, 21, 43), no significant change in channel activity was elicited by heat (Fig. 3E). Fig. 3F shows mean channel activity in response to heat and plotted *versus* time after addition of warm solutions in the presence or absence of PIP_2. The TRPV4 Q_{10} obtained from excised patches containing TRPV4-WT in the presence of PIP_2 was 21±5 (n=3) (Fig. S7B), consistent with previous values obtained from TRPV4 whole-cell recordings (21, 43). Together these experiments confirm that PIP_2 is required for TRPV4 activation by physiological stimuli, probably acting as an allosteric modulator. However, at present we do not have a comprehensive model to incorporate all factors involved in TRPV4 gating, i.e., why TRPV4 gating by 4α−PDD is not affected by PIP_2 depletion or why PIP_2 is unable to activate TRPV4 on its own.

PIP_2 interacts with the TRPV4 N-tail. To further characterize PIP_2 interaction with the TRPV4 N-tail, we carried out limited proteolysis assays on the purified TRPV4 N-terminal region (residues 1-397), which includes the N-terminal tail and the ankyrin repeats. Papain digestion led to cleavage at four positions within the N-tail (Fig. 4A). Quantification of the bands obtained (Fig. 4B-E) showed that proteolysis of TRPV4 N-terminus is reduced in the presence of PIP_2 but not PI. PIP_2-dependent proteolysis protection was not observed with the isolated TRPV4 ankyrin repeats (residues 136-397), the TRPV1 ankyrin repeats or the TRPV4-^{121}AAWAA N-terminal region (Fig. S8), ruling out non-specific inhibition of papain by PIP_2. These biochemical data therefore support a direct interaction of PIP_2 with the N-tail region of TRPV4-WT.

PACSIN3 F-BAR domain is required for TRPV4 channel regulation. The effect of neutralizing the positively charged residues, or depleting PIP_2 levels, on channel activity resembled the response of TRPV4 when coexpressed with PACSIN3, i.e., reduced channel response to hypotonicity and heat but normal response to 4α-PDD (25, 44). PACSIN3 belongs to a family of proteins that contain a Bin-Amphiphysin-Rvs (BAR) domain required to penetrate and remodel the plasma membrane (45, 46). PACSIN3 binds through its SRC homology 3 (SH3) domain to the PRD of TRPV4 (44), in the close proximity of the PI-site. Two competing hypotheses are that membrane-bound PACSIN3 binding to the PRD may either promote or physically block the interaction

of the PI-site with membrane PIP_2. To test these hypotheses, we generated a PACSIN3 lacking the F-BAR domain. Similar deletion in PACSIN1 renders the protein unable to interact with the lipids of the plasma membrane (47). The F-BAR domain of PACSIN3 is not required for interaction with TRPV4 (44). Accordingly, we detected interaction of PACSIN3-ΔF-BAR with TRPV4 (Fig. S9). Coexpression of TRPV4 with PACSIN3-ΔF-BAR, unlike coexpression with PACSIN3, did not reduce the whole-cell currents generated by hypotonic challenges (Fig. 5A). The channel response to 4α-PDD was not affected under any of the experimental conditions tested (Fig. 5B). These results were therefore consistent with the hypothesis that PACSIN3 interferes with the interaction of TRPV4 with PIP_2, an effect that was lost when a membrane-unbound PACSIN3-ΔF-BAR was used.

PIP_2 rearranges TRPV4 cytosolic tails. Together, our findings underscore the involvement of PIP_2 in TRPV4 gating by physiological stimuli. However, an important question remained that has not been resolved for any PIP_2-modulated TRP channel yet. Does PIP_2 binding affect the structural conformation of TRPV4? We approached this question studying the impact of TRPV4 deletions and mutations on the conformation of cytosolic tails. For that purpose we evaluated the proximity of the intracellular C-tails of CFP- and YFP-tagged TRPV4 proteins, which we assumed formed a random population of heteromeric channels, by fluorescence resonance energy transfer (FRET). We tagged C-tails, which remained unmodified in all the TRPV4 deletions/mutations generated, to avoid possible FRET artifacts generated by the different lengths of the N-tails. The relative CFP and YFP fluorescence intensities in the plasma membrane were determined for every single cell and used to calculate FRET efficiencies in transiently transfected HEK-293 cells (Fig. 5C). TRPV4-WT generated a FRET ratio similar to that previously reported (48) while TRPV4-Δ1-130 and TRPV4-^{121}AAWAA doubled the FRET ratio, indicating a more compacted tail conformation. Similarly, coexpression of TRPV4-WT with PACSIN3 markedly increased the FRET signal, an effect that was lost when coexpressed with PACSIN3-ΔF-BAR. We reasoned that the increased FRET observed with mutant TRPV4 proteins or when coexpressed with PACSIN3 was due to the inability of TRPV4 to interact with membrane PIP_2. To test this hypothesis, we studied how the reduction in PIP_2 levels affected FRET efficiency of TRPV4-WT. We overexpressed CFP- and YFP-tagged TRPV4-WT channels in HEK293 cells engineered with tetracycline-inducible expression of 5-phosphatase IV (33). Induction of this enzyme depleted PIP_2 from the plasma membrane (Fig. S5D) and significantly increased FRET ratio (Fig. 5D). This observation further supported the hypothesis that conditions that prevented the N-tail access to membrane PIP_2 (by deletion/mutation of the PI-site or by overexpression of PACSIN3) or depleted PIP_2 from the plasma membrane rearranged the cytosolic TRPV4 tails into a more compacted conformation (increased FRET ratio). Thus, in the presence of PIP_2 and an intact PI-site the intracellular tails appeared in an expanded conformation.

Conclusions. Together, our data provide several new findings. First, we have demonstrated that TRPV4, as many other TRP channels, is regulated by PIP_2, a process that involves PIP_2 binding to a PI-site (^{121}KRWRK^{125}) in the N-tail. Second, we have showed that PIP_2 regulates channel activity in a stimulus-dependent manner. Third, TRPV4 is *bona fide* thermosensitive channel, providing there is PIP_2 to interact with the N-tail. Fourth, the interaction of the TRPV4 PI-site with plasma membrane PIP_2 favors an expanded conformation of the intracellular tails and channel activation by hypotonicity and heat. Conditions that reduced PIP_2 levels (inducible phosphatase) or interfere the interaction of TRPV4 with PIP_2 (mutations in the PI-site or coexpression with PACSIN3) promote a compacted tail conformation and prevent channel activation by hypotonicity and heat. Our study provides the first piece of evidence suggesting that, similar to PIP_2 regulated K^+ channels, PIP_2 interaction with TRPV4 channel rearranges the cytosolic domains. Whether the intracellular tail rearrangement occurring upon PIP_2 binding to TRPV4 facilitates the access of stimuli-generated messengers (e.g., EET) to their binding sites or favors the stimulus-dependent opening of the gates themselves it is not known at present.

MATERIALS AND METHODS

Cells and transfection

For electrophysiological or calcium imaging experiments HeLa or HEK-293 cells were transiently transfected as previously described (16, 48). Primary cultures of tracheal and oviductal ciliated cells were obtained as previously described (7, 17). Animals were maintained and experiments were performed according to the guidelines issued by the Institutional Ethics Committee of the Universitat Pompeu Fabra.

Solutions

Isotonic bath solutions used for imaging experiments contained (in mM): 140 NaCl, 2.5 KCl, 1.2 $CaCl_2$, 0.5 $MgCl_2$, 5 glucose and 10 HEPES, pH 7.3 with Tris. Bath solutions for whole cell recordings contained (in mM): 100 NaCl, 1 $MgCl_2$, 6 CsCl, 10 HEPES, 1 EGTA and 5 glucose, pH 7.3 with Tris. Osmolarity was adjusted to 310 mOsm using mannitol. 30% and 15% hypotonic solutions (255 and 220 mOsm) were obtained by removing mannitol. Whole-cell pipette solution contained (in mM): 20 $CsCl_2$, 100 CsAcetate, 1 MgCl2, 0.1EGTA, 10 HEPES, 4 Na_2ATP and 0.1 NaGTP; 300 mOsm, pH 7.25. Bath and pipette solutions for excised inside-out single channel recordings contained (in mM): 130 CsCl, 1 $MgCl_2$, 1 Na_2ATP, 0.034 $CaCl_2$, 5 EGTA, 10 HEPES (310 mosmol/liter, pH 7.25). When required, solutions were warmed using a water jacket device (Warner Instruments). All chemicals were obtained from Sigma-Aldrich except diC8-PI and diC8-PI(4,5)P2 (Echelon Biosciences Inc.), HC-067047 (Tocris Biosciences) and Fura-2 (Invitrogen).

Electrophysiological and Ratiometric Ca^{2+} recordings

Patch-clamp whole-cell and single single-channel currents were recorded at room temperature (~24ºC, unless otherwise indicated) as previously described (16, 48). Cells/excised patches were perfused at 0.8 ml/min. Cytosolic Ca^{2+} signals, relative to the ratio (340/380) measured prior to cell stimulation, were obtained from cells loaded with 4.5 μM fura-2 AM as previously described (4).

FRET measurements

FRET measurements were carried out in a Leica TCS SP2 confocal microscope (Leica) attached to an inverted microscope. FRET efficiencies expressed as the increase of the FRET donor CFP after bleaching the FRET acceptor YFP (48).

Lipid protection assay

Human TRPV4 ankyrin repeats (136-397) and N-tail (1-397) were cloned using NdeI and NotI into pET21-C6H (49). Recombinant proteins were produced and purified as described (50), except the size exclusion chromatography buffer was 10 mM Tris-HCl pH 7.0, 300 mM NaCl, 10 % glycerol, and 1 mM DTT for TRPV4 N-tail, and 10 mM Tris-HCl pH 7.0, 150 mM NaCl and 1 mM DTT for TRPV4 ankyrin repeats.

Lipid protection assay by limited proteolysis was performed at 4°C (on ice) in reaction buffer containing (in mM): 180 NaCl, 20 Tris-HCl pH 7.0, 1 % glycerol and 1 DTT (for TRPV4-1-397) or 150 NaCl, 20 Tris-HCl pH 7.0 and 1 DTT (for TRPV4-136-397 and TRPV1-ARD). Proteins were pre-incubated in the absence or presence of PI or PIP_2 at 4°C for 60 min and then digested with papain. Final concentrations of protein, lipid, and papain were 10 μM, 150 μM and 38 nM, respectively. Digestion was stopped at 15, 30, 45 and 60 min by adding SDS sample buffer, and samples separated by SDS-PAGE and visualized by Coomassie staining. The gels were scanned and signals were quantified with ImageJ.

Statistical analysis

Data are expressed as mean±SEM (or mean±S.D. in Fig. 4) of n experiments. Statistical analysis was assessed with Student's unpaired test or one-way analysis of variance (ANOVA) using Sigma-Plot software.

Acknowledgments.

We thank Dr T. Voets (KU Leuven, Belgium) for the gift of HEK-293 tetracycline-inducible phosphatase expressing cells, Dr. T. Meyer (Stanford, U.S.A.) for rapamycin-inducible phosphatases and Dr. M. Schaefer (Leipzig, Germany) for help with initial FRET experiments. This work was supported by the Spanish Ministry of Science and Innovation (SAF2012-38140); Fondo de Investigación Sanitaria (Red HERACLES RD12/0042/0014); FEDER Funds; Generalitat de Catalunya (SGR05-266); and National Institutes of Health (R01GM081340). M.A.V. is the recipient of an ICREA Academia Award and U.A.H. of an EMBO Long-Term Fellowship. **Footnotes** [1] A.G-E. and S.M. contributed equally to this work. [2] To whom correspondence should be addressed. E-mail: miguel.valverde@upf.edu Author contributions: A.G-E., R.G., R.V. and M.A.V. designed research; A.G-E, S.M., C.P-P, H.I., F.R-M., C.P.,U.A.H. and R.V. performed research; A.G-E, S.M., C.P-P., H.I., U.A.H. and M.A.V. analyzed data; and M.A.V. wrote the paper. All authors collaborated in paper edition. The authors declare no conflict of interest. This article contains supporting information online

1. Strotmann R, Harteneck C, Nunnenmacher K, Schultz G, Plant TD (2000) OTRPC4, a nonselective cation channel that confers sensitivity to extracellular osmolarity. *Nat Cell Biol* 2:695-702.
2. Liedtke W *et al.* (2000) Vanilloid receptor-related osmotically activated channel (VR-OAC), a candidate vertebrate osmoreceptor. *Cell* 103:525-535.
3. Wissenbach U, Bodding M, Freichel M, Flockerzi V (2000) Trp12, a novel Trp related protein from kidney. *FEBS Lett* 485:127-134.
4. Arniges M, Vazquez E, Fernandez-Fernandez JM, Valverde MA (2004) Swelling-activated Ca^{2+} entry via TRPV4 channel is defective in cystic fibrosis airway epithelia. *J Biol Chem* 279:54062-54068.
5. Suzuki M, Mizuno A, Kodaira K, Imai M (2003) Impaired pressure sensation in mice lacking TRPV4. *J Biol Chem* 278:22664-22668.
6. Liedtke W, Tobin DM, Bargmann CI, Friedman JM (2003) Mammalian TRPV4 (VR-OAC) directs behavioral responses to osmotic and mechanical stimuli in Caenorhabditis elegans. *Proc Natl Acad Sci U S A* 100 Suppl 2:14531-14536.
7. Andrade YN *et al.* (2005) TRPV4 channel is involved in the coupling of fluid viscosity changes to epithelial ciliary activity. *J Cell Biol* 168:869-874.
8. Guler AD *et al.* (2002) Heat-evoked activation of the ion channel, TRPV4. *J Neurosci* 22:6408-6414.
9. Fernandez-Fernandez JM *et al.* (2008) Functional coupling of TRPV4 cationic channel and large conductance, calcium-dependent potassium channel in human bronchial epithelial cell lines. *Pflugers Arch* 457:149-159.
10. Liedtke W. and Friedman JM (2003) Abnormal osmotic regulation in trpv4-/- mice. *Proc Natl Acad Sci U S A* 100:13698-13703.
11. Vriens J *et al.* (2005) Modulation of the Ca^{2+} Permeable Cation Channel TRPV4 by Cytochrome P450 Epoxygenases in Vascular Endothelium. *Circ Res* 97:908-915.
12. Earley S, Heppner TJ, Nelson MT, Brayden JE (2005) TRPV4 forms a novel Ca^{2+} signaling complex with ryanodine receptors and BKCa channels. *Circ Res* 97:1270-1279.
13. Alessandri-Haber N, Dina OA, Joseph EK, Reichling D, Levine JD (2006) A transient receptor potential vanilloid 4-dependent mechanism of hyperalgesia is engaged by concerted action of inflammatory mediators. *J Neurosci* 26:3864-3874.
14. Cohen DM (2005) TRPV4 and the mammalian kidney. *Pflugers Arch* 451:168-175.
15. Gevaert T *et al.* (2007) Deletion of the transient receptor potential cation channel TRPV4 impairs murine bladder voiding. *J Clin Invest* 117:3453-3462.
16. Fernandes J *et al.* (2008) IP3 sensitizes TRPV4 channel to the mechano- and osmotransducing messenger 5'-6'-epoxyeicosatrienoic acid. *J Cell Biol* 181:143-155.
17. Lorenzo IM, Liedtke W, Sanderson MJ, Valverde MA (2008) TRPV4 channel participates in receptor-operated calcium entry and ciliary beat frequency regulation in mouse airway epithelial cells. *Proc Natl Acad Sci U S A* 105:12611-12616.
18. Muramatsu S *et al.* (2007) Functional gene screening system identified TRPV4 as a regulator of chondrogenic differentiation. *J Biol Chem* 282:32158-32167.
19. Masuyama R *et al.* (2008) TRPV4-mediated calcium influx regulates terminal differentiation of osteoclasts. *Cell Metab* 8:257-265.
20. Vriens J *et al.* (2004) Cell swelling, heat, and chemical agonists use distinct pathways for the activation of the cation channel TRPV4. *Proc Natl Acad Sci U S A* 101:396-401.
21. Watanabe H *et al.* (2002) Heat-evoked activation of TRPV4 channels in a HEK293 cell expression system and in native mouse aorta endothelial cells. *J Biol Chem* 277:47044-47051.
22. Loukin S, Zhou X, Su Z, Saimi Y, Kung C (2010) Wild-type and brachyolmia-causing mutant TRPV4 channels respond directly to stretch force. *J Biol Chem* 285:27176-27181.
23. Strotmann R, Schultz G, Plant TD (2003) Ca^{2+}-dependent potentiation of the nonselective cation channel TRPV4 is mediated by a C-terminal calmodulin binding site. *J Biol Chem* 278:26541-26549.
24. Phelps CB, Wang RR, Choo SS, Gaudet R (2010) Differential regulation of TRPV1, TRPV3, and TRPV4 sensitivity through a conserved binding site on the ankyrin repeat domain. *J Biol Chem* 285:731-740.
25. D'hoedt D *et al.* (2008) Stimulus-specific modulation of the cation channel TRPV4 by PACSIN 3. *J Biol Chem* 283:6272-6280.
26. Garcia-Elias A, Lorenzo IM, Vicente R, Valverde MA (2008) IP_3 receptor binds to and sensitizes TRPV4 channel to osmotic stimuli via a calmodulin-binding site. *J Biol Chem* 283:31284-31288.
27. Vriens J, Owsianik G, Janssens A, Voets T, Nilius B (2007) Determinants of 4α-phorbol sensitivity in transmembrane domains 3 and 4 of the cation channel TRPV4. *J Biol Chem* 282:12796-12803.
28. Verma P, Kumar A, Goswami C (2010) TRPV4-mediated channelopathies. *Channels (Austin)* 4:319-328.
29. Nilius B, Owsianik G, Voets T (2008) Transient receptor potential channels meet phosphoinositides. *EMBO J* 27:2809-2816.
30. Rohacs T (2009) Phosphoinositide regulation of non-canonical transient receptor potential channels. *Cell Calcium* 45:554-565.
31. Prescott ED and Julius D (2003) A modular PIP_2 binding site as a determinant of capsaicin receptor sensitivity. *Science* 300:1284-1288.
32. Brauchi S *et al.* (2007) Dissection of the components for PIP2 activation and thermosensation in TRP channels. *Proc Natl Acad Sci U S A* 104:10246-10251.
33. Nilius B *et al.* (2006) The Ca^{2+}-activated cation channel TRPM4 is regulated by phosphatidylinositol 4,5-biphosphate. *EMBO J* 25:467-478.
34. Lukacs V *et al.* (2007) Dual regulation of TRPV1 by phosphoinositides. *J Neurosci* 27:7070-7080.
35. Hansen SB, Tao X, MacKinnon R (2011) Structural basis of PIP2 activation of the classical inward rectifier K+ channel Kir2.2. *Nature* 477:495-498.
36. Whorton MR.and MacKinnon R (2011) Crystal structure of the mammalian GIRK2 K+ channel and gating regulation by G proteins, PIP2, and sodium. *Cell* 147:199-208.
37. Tian W *et al.* (2009) A loss-of-function nonsynonymous polymorphism in the osmoregulatory TRPV4 gene is associated with human hyponatremia. *Proc Natl Acad Sci U S A* 106:14034-14039.
38. Gamper N and Rohacs T (2012) Phosphoinositide sensitivity of ion channels, a functional perspective. *Subcell Biochem* 59:289-333.
39. Suh BC, Inoue T, Meyer T, Hille B (2006) Rapid chemically induced changes of PtdIns(4,5)P2 gate KCNQ ion channels. *Science* 314:1454-1457.
40. Rohacs T, Lopes CM, Michailidis I, Logothetis DE (2005) PI(4,5)P2 regulates the activation and desensitization of TRPM8 channels through the TRP domain. *Nat Neurosci* 8:626-634.
41. Watanabe H *et al.* (2003) Anandamide and arachidonic acid use epoxyeicosatrienoic acids to activate TRPV4 channels. *Nature* 424:434-438.
42. Everaerts W *et al.* (2010) Inhibition of the cation channel TRPV4 improves bladder function in mice and rats with cyclophosphamide-induced cystitis. *Proc Natl Acad Sci U S A* 107:19084-19089.
43. Chung MK, Lee H, Caterina MJ (2003) Warm temperatures activate TRPV4 in mouse 308 keratinocytes. *J Biol Chem* 278:32037-32046.
44. Cuajungco MP *et al.* (2006) PACSINs bind to the TRPV4 cation channel. PACSIN 3 modulates the subcellular localization of TRPV4. *J Biol Chem* 281:18753-18762.
45. Wang Q *et al.* (2009) Molecular mechanism of membrane constriction and tubulation mediated by the F-BAR protein Pacsin/Syndapin. *Proc Natl Acad Sci U S A* 106:12700-12705.
46. Plomann M, Wittmann JG, Rudolph MG (2010) A hinge in the distal end of the PACSIN 2 F-BAR domain may contribute to membrane-curvature sensing. *J Mol Biol* 400:129-136.
47. Plomann, M., Mörgelin, M. & Schael.S. (2009) in *The Pombe Cdc15 Homology Proteins*, ed. Aspenström, P. (Landes Biosciences, Austin), pp. 39-48.
48. Arniges M, Fernandez-Fernandez JM, Albrecht N, Schaefer M, Valverde MA (2006) Human TRPV4 channel splice variants revealed a key role of ankyrin domains in multimerization and trafficking. *J Biol Chem* 281:1580-1586.
49. Jin X, Touhey J, Gaudet R (2006) Structure of the N-terminal ankyrin repeat domain of the TRPV2 ion channel. *J Biol Chem* 281:25006-25010.
50. Inada H, Procko E, Sotomayor M, Gaudet R (2012) Structural and biochemical consequences of disease-causing mutations in the ankyrin repeat domain of the human TRPV4 channel. *Biochemistry* 51:6195-6206.

Please review all the figures in this paginated PDF and check if the figure size is appropriate to allow reading of the text in the figure.

If readability needs to be improved then resize the figure again in 'Figure sizing' interface of Article Sizing Tool.

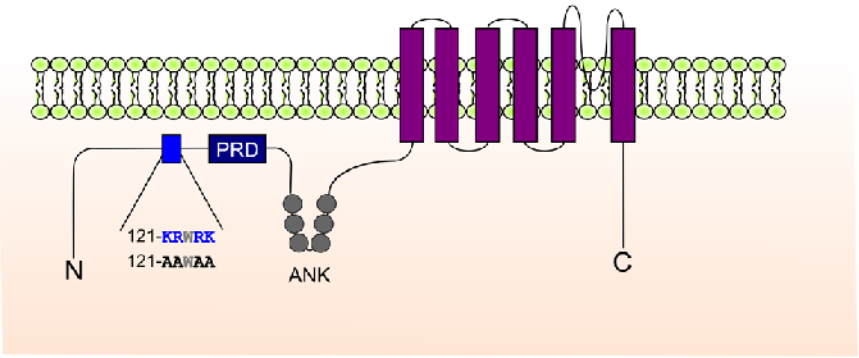

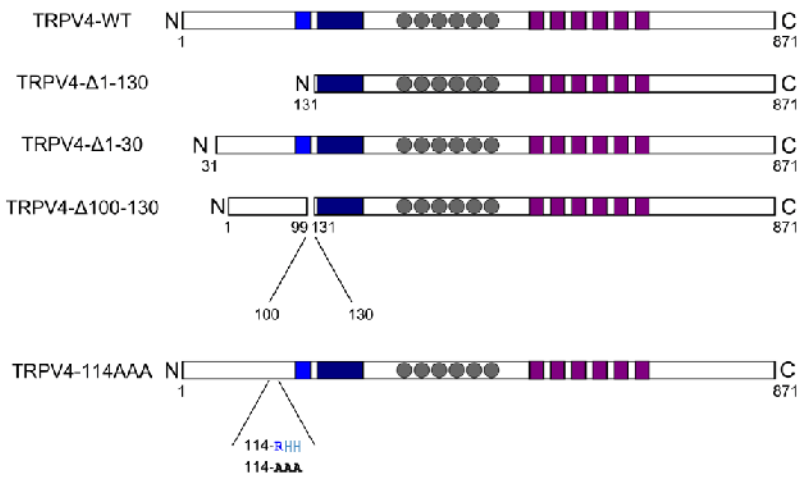

Figure S1. Schematic representation of the TRPV4 channel with the deletions and mutations used in this study. PRD, Proline Rich Domain. ANK, ankyrin repeats.

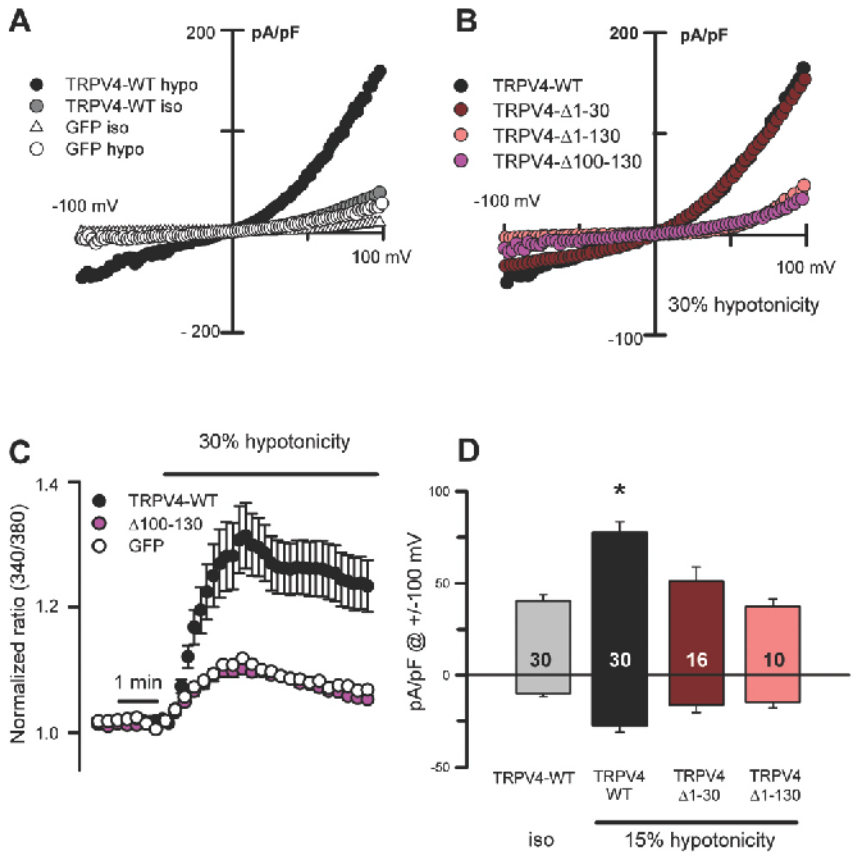

Figure S2. Functional analysis of N-terminal truncations of TRPV4. (A) Ramp current-voltage relations of cationic currents recorded from HEK-293 cells transfected with TRPV4-WT or GFP and exposed to isotonic and 30% hypotonic solutions. (B) Ramp current-voltage relations of cationic currents recorded from HEK-293 cells transfected with TRPV4-WT, TRPV4-Δ1-30, TRPV4-Δ1-130, TRPV4-Δ100-130 and exposed to 30% hypotonic solutions. Representative traces in (A-B) correspond to the average values shown in Fig. 1A of the main text. (C) Calcium signals (fura-2 ratio) obtained in HeLa cells transfected with TRPV4-WT (n=50) or TRPV4-Δ100-130 (n=70) and GFP (n=37) exposed to 30% hypotonic solutions. All cells analyzed were included. (D) Mean current density measured at +100 and -100 mV recorded from cells transfected with TRPV4-WT, TRPV4-Δ1-30 and TRPV4-Δ1-130 exposed to 15% hypotonic solutions Number of cells recorded is shown for each condition. Mean±S.E.M. * $P<0.05$, one way ANOVA and Bonferroni *post hoc*.

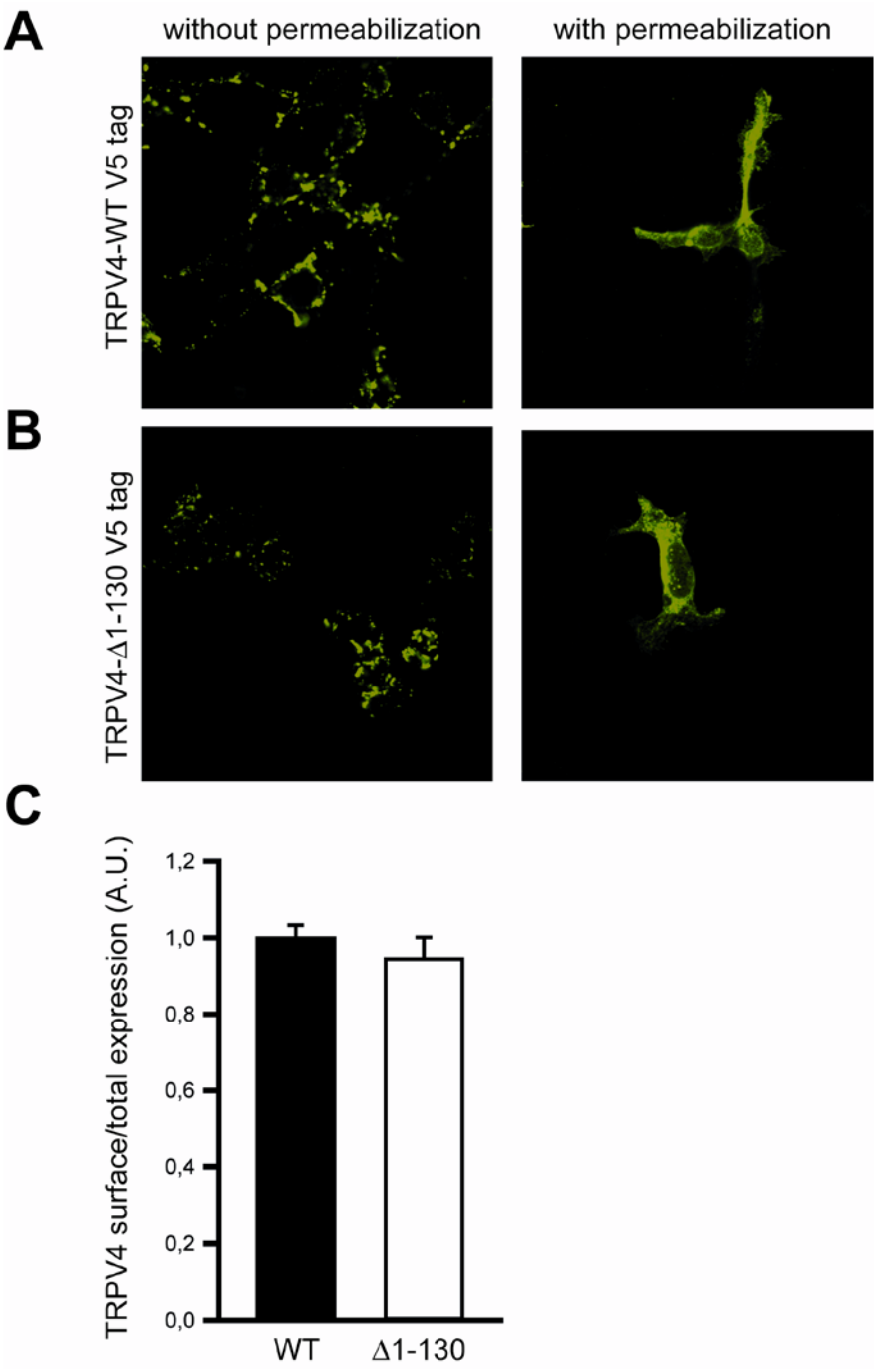

Figure S3. Membrane localization of TRPV4-WT and TRPV4-Δ1-130. (A), Confocal immunofluorescence images of non-permeabilized (left) and permeabilized (right) HEK-293 cells overexpressing TRPV4-WT tagged with V5 in the first extracellular loop. (B), Confocal immunofluorescence images of non-permeabilized (left) and permeabilized (right) HEK-293 cells overexpressing TRPV4-Δ1-130 tagged with V5 in the first extracellular loop. (C), Quantification of surface expression (normalized to total cell expression) of V5 tagged TRPV4-WT (n=9) and TRPV4-Δ1-130 (n=9) using an HRP-linked secondary antibody and chemiluminiscence analysis.

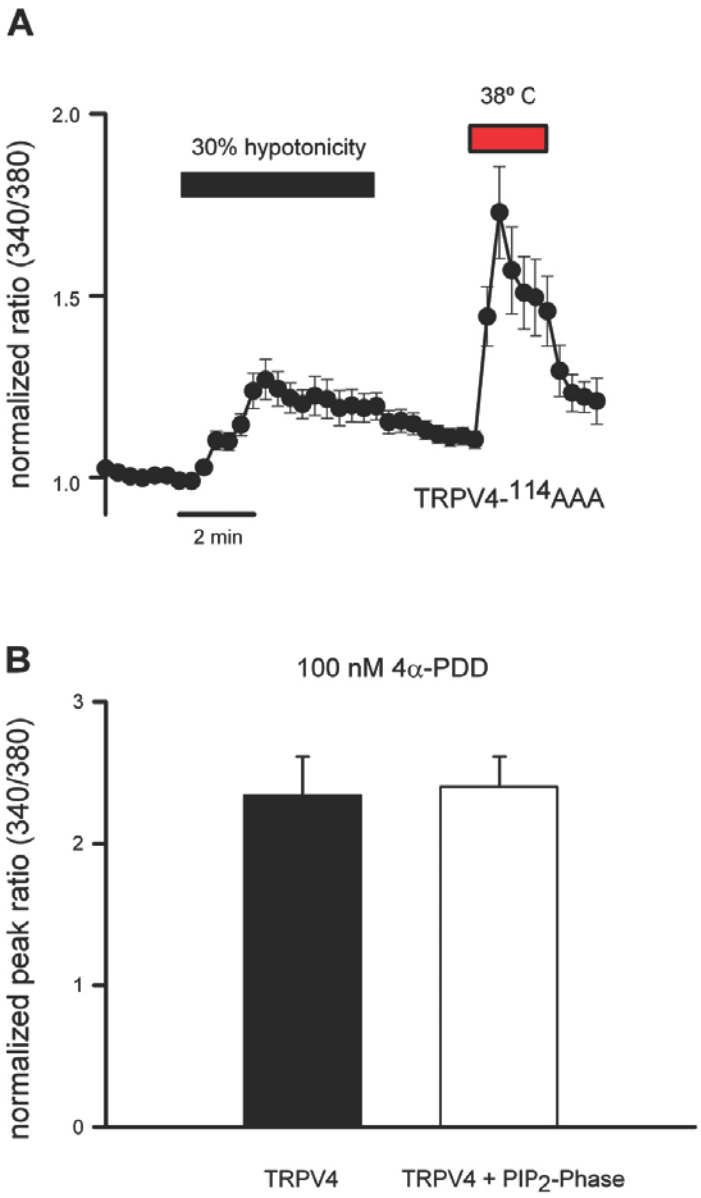

Figure S4. Functional analysis of TRPV4-^{114}AAA. (A) Calcium signals (fura-2 ratio) obtained in HeLa cells transfected with TRPV4-^{114}AAA and sequentially stimulated with 30% hypotonic solutions and heat (38° C). Mean±S.E.M., n=133. (B) Peak calcium signals measured in HeLa cells cotransfected with TRPV4-WT, FRB and FKBP-5-phosphatase (PIP_2-ptase) and exposed to 100 nM 4α-PDD. Cells were pretreated with the phosphatase translocation inducing agent rapamycin (1 μM). TRPV4 (n=43), TRPV4 +PIP_2-Phase (n=46).

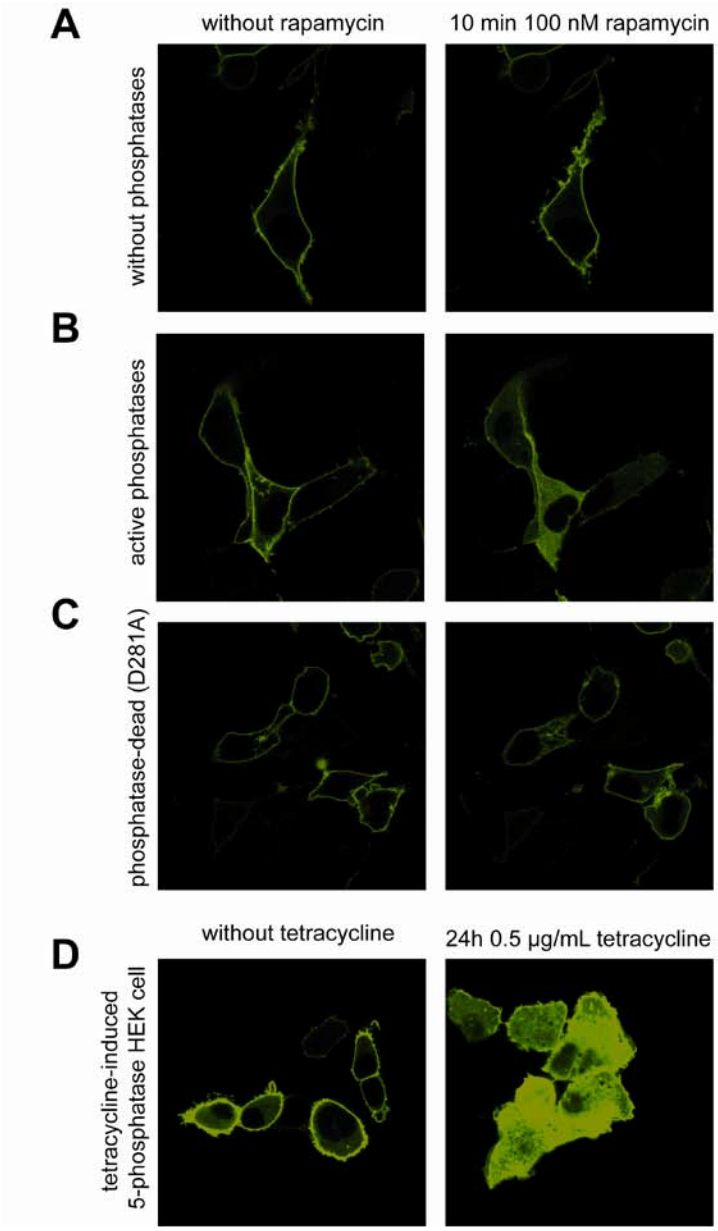

Figure S5. Trasnlocation PH-PLC. (A-C) Confocal images of HeLa cells expressing a yellow fluorescent protein (YFP)–tagged pleckstrin homology (PH) domain from phospholipase C–δ1 (PLC-δ1) serving as a PIP_2 biosensor (YFP-PH(PLC-δ)), the rapamycin-binding protein FRB and either the cytoplasmic enzyme construct FKBP-5-phosphatase (PIP_2-ptase) or the inactive phosphatase (D281A). Images were taken in the absence (left, mainly plasma membrane signal) or presence (right, cytosolic signal) of the phosphatase translocation inducing agent rapamycin (1 µM). (D), Depletion of PIP_2 in HEK-293 cells overexpressing a tetracycline-induced 5-phosphatase. Left, cells without treatment with tetracycline (no 5-phosphatase induction). Right, images obtained 24h after induction of 5-phosphatase with 0.5 µg/mL tetracycline.

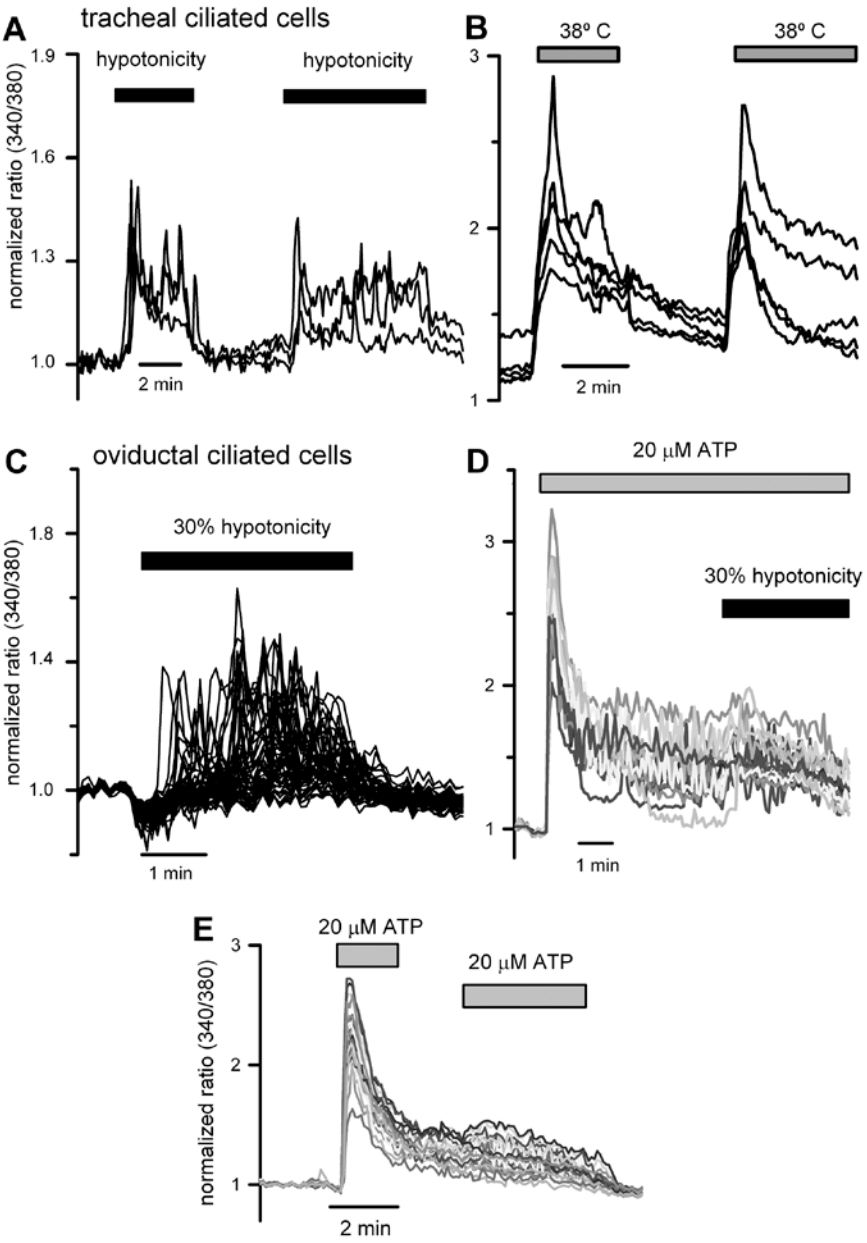

Figure S6. Ciliated epithelial cells response to hypotonic cell swelling and heat. (A-B) Representative traces of the intracellular calcium signals obtained from mouse tracheal ciliated cells exposed to two consecutive hypotonic solutions (A) or heat stimuli (B). (C-D) Representative traces of the intracellular calcium signals obtained from mouse oviductal ciliated cells exposed to hypotonic solutions in the absence (C) or in the presence (D) of previous activation of G-protein-coupled purinergic receptors with ATP (20 μM). Note the almost complete absence of response to hypotonicity following exposure to ATP. (E) Second, within mins, stimulation with ATP did not trigger intracellular calcium signals in mouse oviductal ciliated cells.

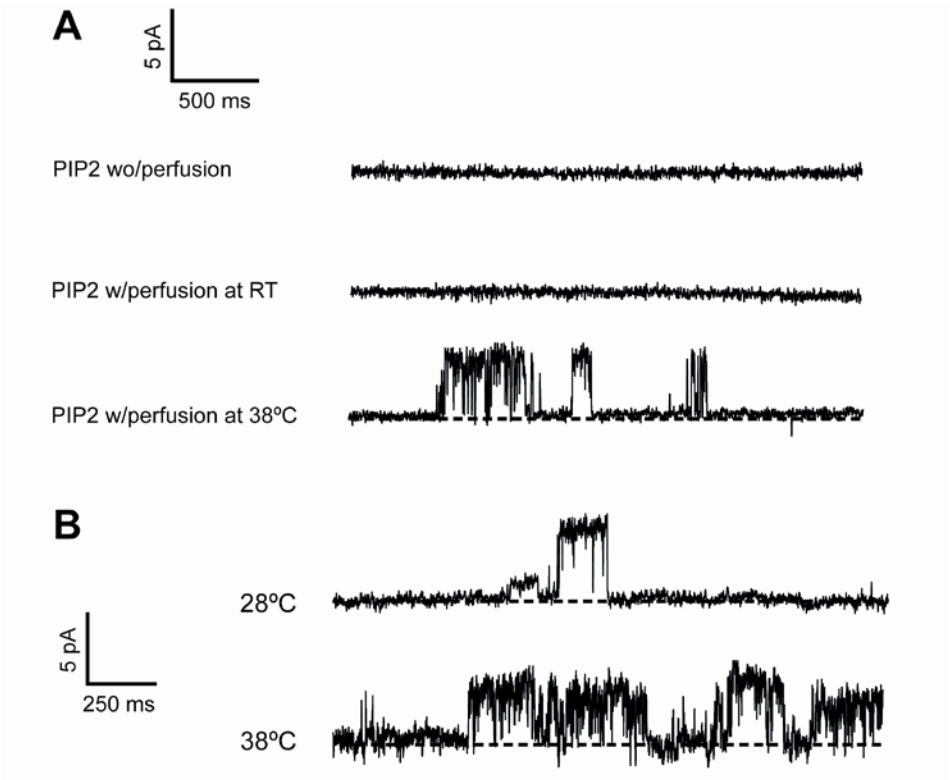

Figure S7. Heat activation of TRPV4 channel in inside-out patches. (A) Activation of TRPV4 channel in the presence of PIP_2 was not triggered by the shear stress generated by the flow of the external solution, but by the increase in temperature. (B) To calculate the Q_{10} of the TRPV4 channel the same excised patch was first exposed to 28ºC and then to 38ºC.

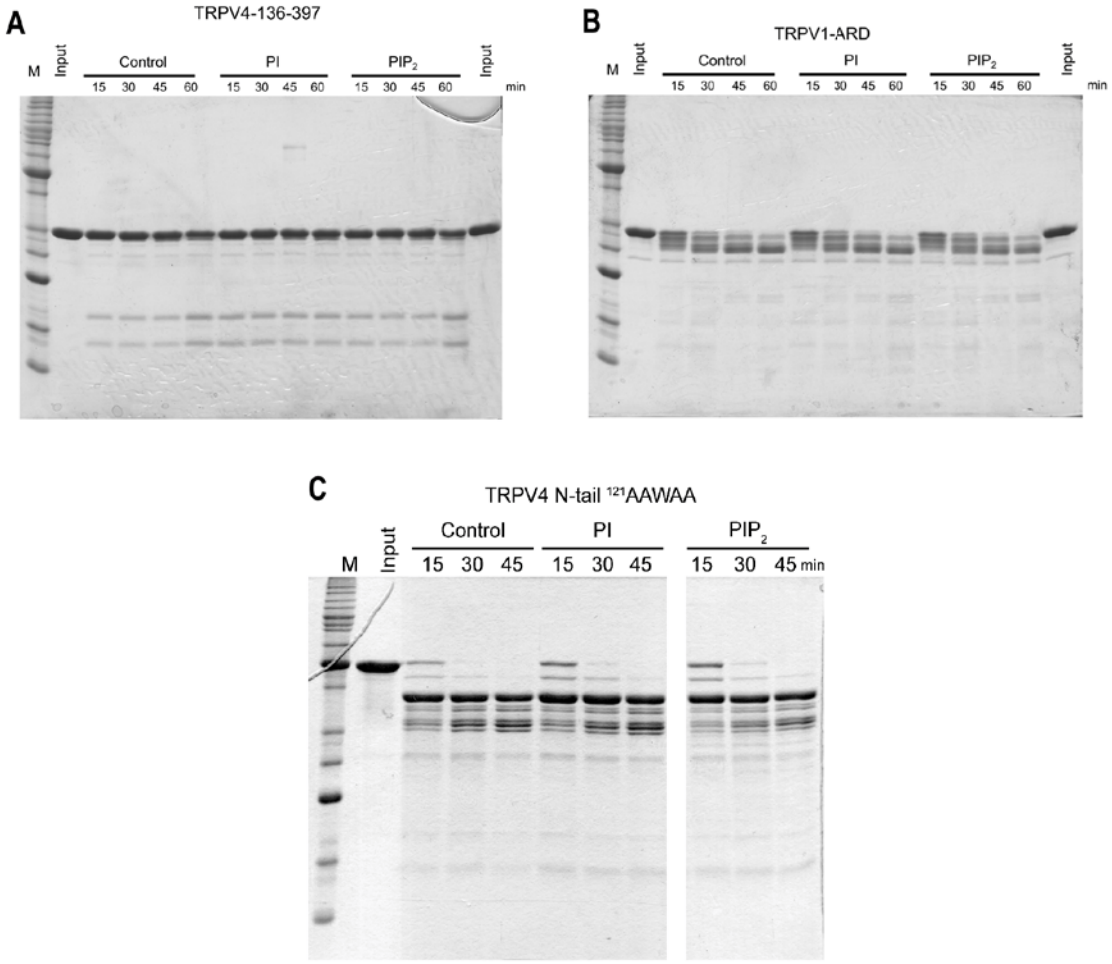

Figure S8. Differential proteolysis protection of the TRPV4 N-terminus by different phosphoinositides and dependence on the ^{121}KRWRK^{125} motif. (A) Analysis of PIP_2-mediated proteolysis protection of the human TRPV4 N-tail lacking residues 1-135. Coomassie-stained SDS-PAGE of TRPV4 samples after 15, 30, 45 and 60 min digestion with papain in the absence or presence of PI or PIP_2. (B) Analysis of PIP_2-mediated proteolysis protection of the rat TRPV1 ankyrin repeats (residues 101-364). Coomassie-stained SDS-PAGE of TRPV1 samples obtained after 15, 30, 45 and 60 min digestion with papain in the absence or presence of PI or PIP_2. (C), Coomassie-stained SDS-PAGE of TRPV4-^{121}AAWAA N-tail samples obtained after 15, 30 and 45 min digestion with papain in the absence or presence of PI or PIP_2, showing that none of the phosphoinosides protect the mutant from proteolysis. These gels are representative results from four similar experiments

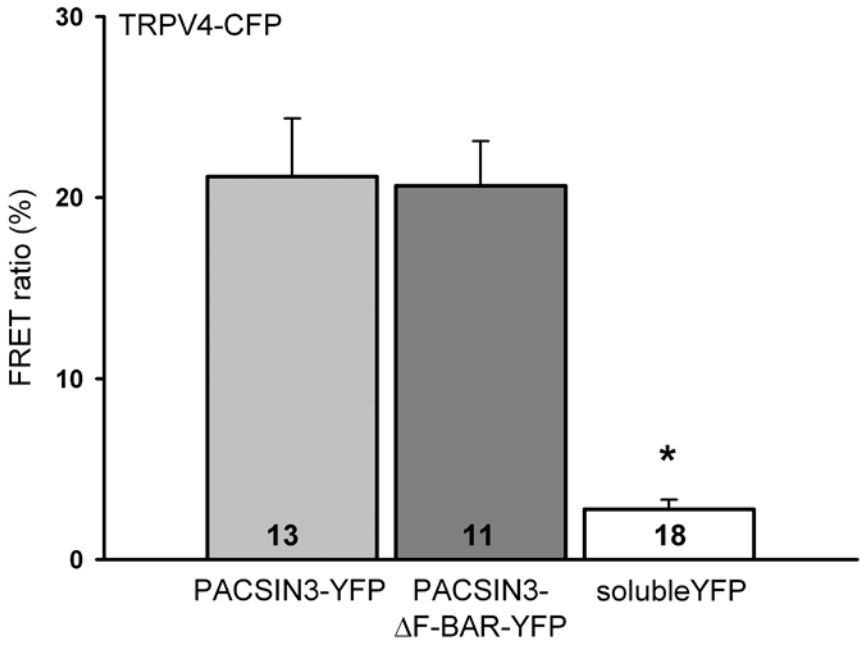

Figure S9. Interaction of TRPV4 with PACSIN3. FRET ratios, represented as the CFP increase during YFP photobleaching normalized to the initial CFP value, determined at the plasma membrane of HEK-293 cells expressing TRPV4-WT-CFP and either PACSIN3-YFP, PACSIN3-ΔF-BAR or soluble YFP. Number of cells recorded is shown for each condition. Mean±S.E.M. * $P<0.05$, one way ANOVA and Bonferroni *post hoc*.